A peer-reviewed version of this preprint was published in PeerJ on 18 April 2017.

Klein N, Guenther E, Mikus P, Stehling MK, Rubinsky B. 2017. Single exponential decay waveform; a synergistic combination of electroporation and electrolysis (E2) for tissue ablation. PeerJ 5:e3190 https://doi.org/10.7717/peerj.3190

Single exponential decay waveform; a synergistic combination of electroporation and electrolysis (E2) for tissue ablation

Nina Klein [Corresp., 1, 2] , **Enric Guenther** [1, 2] , **Paul Mikus** [1] , **Michael K Stehling** [1, 2] , **Boris Rubinsky** [1, 3]

[1] Inter Science GmbH, Gisikon, Switzerland

[2] Prostata Center, Institut fur Bildgebende Diagnostik, Offenbach, Germany

[3] Department of Mechanical Engineering, University of California, Berkeley, Berkeley, United States

Corresponding Author: Nina Klein
Email address: n.klein@biophysik.org

Background: Electrolytic ablation and electroporation based ablation are minimally invasive, non-thermal surgical technologies that employ electrical currents and electric fields to ablate undesirable cells in a volume of tissue. In this study we explore the attributes of a new tissue ablation technology that simultaneously delivers a synergistic combination of electroporation and electrolysis (E2).

Method: A new device that delivers a controlled dose of electroporation field and electrolysis currents in the form of a single exponential decay waveform (EDW), was applied to the pig liver and the effect of various parameters on the extent of tissue ablation was examined with histology.

Results: Histological analysis shows that E2 delivered as EDW can produce tissue ablation in volumes of clinical significance, using electrical and temporal parameters which, if used in electroporation or electrolysis separately, cannot ablate the tissue

Discussion: The E2 combination has advantages over the three basic technologies of non-thermal ablation: electrolytic ablation, electrochemical ablation (reversible electroporation with injection of drugs) and irreversible electroporation. E2 ablates clinically relevant volumes of tissue in a shorter period of time than electrolysis and electroporation, without the need to inject drugs as in reversible electroporation or use paralyzing anesthesia as in irreversible electroporation.

Single exponential decay waveform; a synergistic combination of electroporation and electrolysis (E2) for tissue ablation

Nina Klein[1,2*], Enric Gunther[1,2*], Paul Mikus[1], Michael Stehling[1,2], Boris Rubinsky[1,3]

[1]Inter Science GmbH, Biophysics, 6038 Gisikon, Luzern, Switzerland
[2]Institut fur bildgebende Diagnostik, Prostata Center, 63067 Offenbach, Germany
[3]Department of Mechanical Engineering, University of California Berkeley, Berkeley CA 84720 USA

Corresponding Author: Nina Klein

E-mail address – n.klein@biophysik.org

Abstract

Background: Electrolytic ablation and electroporation based ablation are minimally invasive, non-thermal surgical technologies that employ electrical currents and electric fields to ablate undesirable cells in a volume of tissue. In this study we explore the attributes of a new tissue ablation technology that simultaneously delivers a synergistic combination of electroporation and electrolysis (E2).

Method: A new device that delivers a controlled dose of electroporation field and electrolysis currents in the form of a single exponential decay waveform (EDW), was applied to the pig liver and the effect of various parameters on the extent of tissue ablation was examined with histology.

Results: Histological analysis shows that E2 delivered as EDW can produce tissue ablation in volumes of clinical significance, using electrical and temporal parameters which, if used in electroporation or electrolysis separately, cannot ablate the tissue

Discussion: The E2 combination has advantages over the three basic technologies of non-thermal ablation: electrolytic ablation, electrochemical ablation (reversible electroporation with injection of drugs) and irreversible electroporation. E2 ablates clinically relevant volumes of tissue in a shorter period of time than electrolysis and electroporation, without the need to inject drugs as in reversible electroporation or use paralyzing anesthesia as in irreversible electroporation.

Keywords

tissue ablation, liver, electrolytic ablation, reversible electroporation, irreversible electroporation, synergy electroporation and electrolysis

Introduction

A number of biophysical and biochemical phenomena occur simultaneously when electrical potentials are applied across biological matter. These include Joule heating due to electrical current energy dissipation, electrolytic reactions at the interface between the electrodes and the biological milieu, and cell membrane permeabilization known as electroporation. All these electrical phenomena are used for tissue ablation. Usually the electrical potential delivery protocol is designed in such a way as to maximize one phenomenon, while minimizing the others. For example, in non-thermal irreversible electroporation (NTIRE) the electrical potential profile is designed to maximize irreversible electroporation while minimizing Joule heating (Davalos et al. 2005). The non-thermal aspect of NTIRE was found to be beneficial in tissue ablation treatments, in which it is desired to spare vital sites in the treated lesion, such as blood vessels and nerves.

In electrolytic tissue ablation, cell death is caused by the chemical interaction between the products of electrolysis and cells (Nilsson et al. 2000),(Czymek et al. 2011). Because the ablation is caused by a chemical reaction, it is a function of compounds concentration and time of exposure. One drawback of tissue ablation by electrolysis is the need for high concentrations of electrolytes and lengthy times of exposure. An advantage is the very low currents and voltages used.

In ablation by electroporation, brief, pulsed, high electric fields are used to permeabilize the cell membrane. Lower electric fields and small numbers of pulses yield reversible electroporation, in which the cell membrane permeabilization is temporary. Higher electric fields with larger number of pulses yield irreversible electroporation in which the cell membrane permeabilization is permanent, which results in cell death. Both reversible and irreversible electroporation are used for tissue ablation, each with their advantages and disadvantages. Reversible tissue electroporation is used for tissue ablation in combination with cytotoxic additives, in a procedure known as electrochemotherapy (Mir et al. 1991), (Marty et al. 2006). One advantage of ablation by means of irreversible electroporation over electrochemotherapy is that no chemotoxic drugs are injected into the tissue (Rubinsky et al. 2007), while the advantage of electrochemotherapy over irreversible electroporation is the use of fewer pulses and lower electric fields. The need to inject cytotoxic additives adds a complicating step to the electrochemotherapy procedure. Cell death through electrochemotherapy is dependent on mitosis cycle rendering and is possibly more tissue selective, while irreversible electroporation induces apoptosis and necrosis instantaneously over the whole volume exposed to sufficiently high fields. However, the high electric fields and the large number of pulses used in conventional irreversible electroporation protocols cause some undesirable effects. They induce muscle contractions that require the use of a muscle relaxant and deep anesthesia during surgery. It should be noticed that in clinical practice, reversible electroporation is mostly used without muscle relaxants and with topical anesthesia (Marty et al. 2006). Every clinical electroporation protocols, reversible or irreversible, generates some products of electrolysis, and some heat. We have recently shown that if substantial amounts of products of electrolysis are inadvertently generated during an

electroporation protocol, a highly detrimental electrical discharge across the layer of gas formed on the electrodes can occur (Guenther et al. 2015).

In several recent papers we have shown that combining electroporation and electrolysis (E2) sagaciously yields a new technology of tissue ablation with certain advantages over tissue ablation by electroporation (reversible or irreversible) or electrolysis alone (Phillips, Raju et al. 2015) (Phillips et al. 2016) (Stehling et al. 2016). We have developed several possible synergistic electroporation and electrolysis (E2) protocols. One effective combination entails delivering first several (eight) reversible electroporation type pulses followed by the injection of a low voltage direct current to generate products of electrolysis. While effective, this combination requires two different power supplies, one for electroporation and the second for electrolysis (Phillips et al. 2015) (Phillips et al. 2016) (Stehling et al. 2016). The combined voltage profile of electroporation pulses followed by low voltage electrolysis reminded us of an exponential decay waveform (EDW), generated by the discharge of a capacitor; a type of pulse which was rather common in the early stages of electroporation research (Sale and Hamilton 1967). The shape of the capacitor discharge exponential decay waveform is a high initial voltage followed by a rapid decay towards a trailing low voltage. This type of waveform is still used in cell electroporation. We thought that with a properly chosen set of capacitor discharge parameters, the initial high voltage over a suitable timeframe could serve for electroporation, while the trailing lower voltage could generate sufficient charge for the generation of electrolytic products. The feasibility of tissue ablation with a EDW, was shown in the liver of a small rodent (Phillips et al. 2016). Here, we extend the study to a large animal model, pig liver, and show that EDW has the ability to ablate tissue volumes of clinical significance. The experimental study was supported by a mathematical analysis to evaluate the electric fields and extent of thermal damage generated by the exponential decay waveform.

Materials and methods:

Animal protocol:

The study was approved by Sir José Antonio Rodríguez Correa, Director of Animal Health Programs and General Director of Department of Agriculture and Livestock, Ministry of Environment and Rural, Agricultural Policies and Territory, Government of Autonomous Community of Extremadura (Spain), with application form number: 2015209030009567 and study register number: 100370001499. The experiment was conducted on *in vivo* pig liver, which was in accordance with Royal Decree Law 53/2013 (Feb.1st). According to the study protocol, three female pigs between 90-110 kg were treated. After being fasted for 24 hours, animals were pre-medicated with a combination of diazepam (0.4mg/kg) and ketamine (15mg/kg) injected intramuscularly (IM). Anesthesia was induced with intravenous (IV) Propofol (3mg/kg). Endotracheal intubation was performed and anesthesia was maintained with sevoflurane in oxygen (adjusted to 1.8-2% End tidal sevoflurane). Possible postoperative pain was treated with

Buprenorphine 0.01 mg/kg IM Pre-med at recovery and Carprofen 4 mg/kg at extubation/recovery. Cefazolin 25 mg/kg IV was administrated every 2 hours. If found to be needed during the procedure, the study had the ability to deliver pancuronium (0.1 mg/kg, at a dose of 1 mg/ml) through an IV to reduce muscle contractions during the application of the electrical pulses. The liver was exposed via a midline incision. The treatment was delivered using two 18-gauge Titanium needles (Inter Science GmbH, Ch) with a variable length (1-4 cm exposed treatment length) insulating sheath inserted in the liver. Titanium was chosen, because, unlike steel or aluminum it is chemically inert, and does not introduce toxic metals in tissue, during the electrolysis stage. In addition, Ti is MRI compatible. The 18-gauge variable length electrodes were custom designed for the delivery of both electroporation and electrolytic pulse sequences.

Two electrodes were inserted in the liver under ultrasound monitoring, in a roughly axial parallel configuration, normal to the liver surface. Ultrasound images were also taken throughout the procedure. Since no apparatus is currently available to produce the exponential decay voltage waveform needed for the SEE procedure conceived by us, we have designed and built a new power supply described in the following device section. The parameters varied in this study were: the initial voltage and the time constants of the exponential voltage waveform. In addition, we varied the number of exponential voltage waveforms delivered. A total of 23 lesions were produced, in three pigs, in separate experiments. Animals were sacrificed at 24 hours. The pigs were euthanized using Euthasol 1 ml/lb IV.

To fix the liver for microscopic viewing, a Foley catheter was placed into the descending aorta and the hepatic vein was snipped off for drainage of the affluent. The liver was flushed with physiological saline for ten minutes at a hydrostatic pressure of 80 mmHg from a pressurized IV drip. Immediately following saline perfusion, a 10% formalin fixative was perfused in the same way for ten minutes. The liver lobe in which the SEE lesion was made was removed and stored in the same formalin solution. For microscopic analysis, the tissue was bread loafed perpendicular to the capsule surface and parallel to the needle tracts. All cassettes were processed routinely from 10% phosphate buffered formalin to wax blocks. Five micrometer sections were made from each block and stained with Masson's trichromatic stain for histologic examination. The stained samples were examined and analyzed by an independent histology service company and reports were prepared (Narayan Raju, Inc, South San Francisco, CA). The focus of the histology was to verify the extent and nature of tissue ablation with E2. To produce information of practical clinical value, the focus of the analysis was on verifying the ability to produce a continuous lesion between the electrodes.

Device

We were unable to find a power supply that can produce the waveform parameters, required for an EDW protocol in tissues with the dimensions of the pig liver. Therefore, we designed a power supply that operates in the modality of capacitor discharge electroporation systems (e.g. Gene Pulser Xcell™ Electroporation System, BioRad, Hercules, CA) with an enhanced performance. The conventional type capacitors used were replaced with a 100 microfarad capacitor to provide the charge required for electrolysis. Similar to the Gene Pulser Xcell™, the generator has an output

of up to 3kV. Because of the larger capacitors it can generate exponential decay waveforms up to time ranges of hundred milliseconds, depending on tissue conductivity and thereby simultaneously deliver electrolysis and electroporation. The apparatus selects and matches the internal components needed to produce the time constants selected for the specific tissue conductivity of the treatment area. The apparatus is able to produce and deliver the exponential decay voltage profile in the time and voltage range for the specific treatment area.

Mathematical Analysis

The thermal and electrical field simulations were performed using a finite element solver (Comsol Multiphysics 5.2) for the Laplace equation (electrical field) and Pennes Bioheat equation, in a way identical to that described in (Davalos et al. 2005). The setup was approximated as two parallel titanium cylinders in a large volume of liver tissue with the parameters shown in Table 1. In case of discharging capacitors, the amount of Joules heating in tissue is prescribed by the dissipation of the charge energy, Q, ($Q=C*U_0$). Therefore, specifying only, the initial voltage (U_0) and capacity (C) is sufficient to simulate the experiment. Permanent tissue damage can occur instantaneously due to temperatures above 90°C, but also chronically with temperatures above 45°C over a period of time depending on cell type and temperature. The latter mechanism is the only effect for pulse-based treatments in the energy magnitude discussed here where distances of more than a millimeter from the electrode could take thermal damage. Therefore, all temperature graphs in the figures show the temperature after 30 seconds of heat dissipation. The waveform delivered to the electrodes was assumed to be a perfect exponential decay in time, t, ($U= U_0*\exp-(t/\tau)$), where U_0 is the initial voltage and the time constant is, τ. The time constant was taken from the experimental data, through the analysis of the voltage trace during the delivery of the waveform.

Results

A series of 23 lesions were generated in experiments in which we studied the effects of the E2 waveform parameters on tissue ablation. The study examined the effects of the initial voltage, the time constant and the number of exponential decay voltage waveforms delivered. To facilitate a systematic and well defined analysis of the E2 phenomenon, we will focus on the results at midline between the two electrodes.

Figure 1 shows results from a series of studies in which the initial voltage between electrodes was 750 V, the distance between electrodes was 15 mm, the exposed length was 10 mm and the depth of penetration was 20 mm. This configuration produces an initial voltage over distance of 500 V/cm. The calculated electrical field norm is displayed in panel A and the calculated temperature in panel B. Geometrically, both graphs represent the 1d-cutline through the perpendicularly induced electrodes with the electrical field and the temperatures respectively on the y-axis. Panels C and D are the macroscopic histology from lesions treated with a voltage difference of 750 V between the electrodes and time constants of 50 ms and 100 ms, respectively. If tissue resistance and conduction between electrode and tissue were constant, the discharge

could be fully described using the time constant of the EDW. However, secondary effects like thin layers of burned tissue, can cause insulation and hence disrupt the ideal exponential decay. This does not necessarily have any negative effect on the ablation, but will limit τ to adequately describe the delivered waveform. The panels show the formalin embedded samples, sectioned in a plane that is transverse to the centers of the two electrodes. In all the different experiments with 750 V (500 V/cm voltage to distance between electrodes) there was no configuration in which the lesion between electrodes became continuous. Panels A and B show that at the line midway between the electrodes the electric field is less than 200 V/cm and the temperature is below 40°C.

Figure 2 shows results from an experiment in which the initial voltage between electrodes was 1000 V, the distance between electrodes was 15 mm, the exposed length was 10 mm, the depth of penetration was 20 mm and the time constant was 70 ms. The slides were prepared with Masson's trichrome staining. Fig A gives an overview of the evaluated slide. The image is taken in a plane that transverses the centers of the two electrodes. The area of the probe is clearly visible, with a deep blue color at the site of the probes, representing the cellular damage caused by thermal necrosis, surrounded by areas of coagulated blood (deep red color). 10x magnification at the anode (Fig 2B) illustrates an area of thermal necrosis, where the hepatocytes have sustained more intense cellular ablation injury resulting in denaturation of the cytoplasmic organelles. At the cathode (Fig 2D) we can witness the gradual effect of the treatment: Around the macroscopically visible lesion there is a pale area which represents less affected cells immediately adjacent to the severely affected hepatocytes (marked with an arrow). The sinusoidal spaces are dilated due to edema and/or hepatocellular swelling, while the nuclei are condensed. The space between the electrodes is not fully ablated, as the microscopic images show areas of unaffected cells (Figure 2C). Figure 2E shows the calculated electric field for a voltage of 1000 V and figure 2F shows the calculated temperature distribution. Panels 2E and 2F show that, for these experimental conditions, the minimal electric field midway between the electrodes is calculated to be about 240 V/cm and the temperature midway between the electrodes is well below 40°C.

Figure 3 illustrates the pathology of liver, from a treatment in which two voltage exponential decay waveforms with similar parameters as those that produced Figure 2, were delivered at an interval of 30 seconds. The macroscopic image taken from a plane between the center of the two electrodes (Fig. 3A) shows that the partial electrode pathway (tunnel) is filled with coagulated blood. This is confirmed by the deep red linear region in the histological slides stained with Masson's trichrome staining in Figure 3B to 3D. The dark blue zone around that region (Figs 3B-3D) represents the more severely ablated hepatocytes, by virtue of being closest to the point of energy release. Figure 3E shows the calculated electric field for an exponential decay waveform with an initial voltage of 1000 V and figure 3F shows the calculated temperature distribution at the onset of the second pulse. There are two aspects to notice in panels 3E and 3F. Figure 3E is a copy of Figure 2E. It is obvious because we have used the electrical parameters of normal liver. However, it is known that the electrical conductivity of electroporated tissue changes after electroporation (Ivorra and Rubinsky 2007), and therefore this panel may not be correct. The second aspect relates to the temperature distribution. Figure 3E shows that the calculated

temperature distribution, when the second pulse is delivered is substantially elevated over the initial temperature when the first pulse is delivered, and thermal damage may be induced near the electrodes.

Figure 4 shows 10x magnified images of the histological slide from Figure 3. Fig. 4A shows the space between the electrodes. Fig. 3B gives a 10x magnification of that area, showing a full ablation zone, with affected cells throughout the area. Hepatocytes both at the cathode (Fig 4C) and anode (Fig 4D) show condensed nuclei, with hemorrhage in the spaces between, however with intact vessels (Fig 4C).

Figure 5 shows the histological results of exponential voltage profile in which the initial voltage between electrodes was 1500 V, the distance between electrodes was 15 mm, the exposed length was 20 mm and the depth of penetration was 30 mm. It is important to notice that the top 10 mm of the electrode was insulated. The slides were prepared with Masson's trichrome staining. Fig 5A shows the cells on the center line between the electrodes at the level of the top 10 mm insulated part of the electrodes. Here we see that the cells are not affected by the treatment. The next panel (Fig. 5B), however, shows the lesion which was caused by the treatment in the uninsulated part of the tissue between the electrodes. The lesion is continuous between electrodes at this level. Figure 5C displays the calculated electric field for a voltage of 1500 V, and figure 5D shows the calculated temperature distribution. The electric field midway between the electrodes is about 550 V/cm. The midway between electrodes temperature is about 40°C.

Figure 6 displays a 10x magnification of the pathological slide shown in Figure 5. Panel 6 A is a magnification of the cathode, showing swollen and necrotic hepatocytes and a disrupted sinusoidal pattern. Between the electrodes (Fig. 6B) a bridged ablation with affected cells was observed, with a complete loss of cellular structure. At the anode (Fig. 6C) there is an affected cellular architecture with hemorrhage. Panels 6A-C show open and undamaged large blood vessels within the treatment field.

A very important observation is that there was no need for muscle paralysis in any of the 23 lesions produced with various E2 protocols. This evaluation is based on the assessment of a physician (MS) with an experience of close to 450 NTIRE procedures in which muscle contraction can occur even with deep muscle relaxations.

Discussion

Our experiment was designed to be performed without a muscle relaxant, however, in such a way as to allow for an immediate use of a muscle relaxant as soon as an undesirable level of muscle contraction is noted. From among the 23 experiments with the exponential decay voltage waveform done in this pig liver study, a muscle contraction requiring the use of a muscle relaxant (pancuronium) was detected in none. In fact, the muscle contraction was negligible, and at times unnoticeable. The E2 treatment was delivered by a physician with an experience of close to 400 irreversible electroporation treatments (MS). It was noted that the observed response is clinically

acceptable and the exponential decay voltage waveform procedure can be carried out without the use of muscle paralyzing drugs. Obviously this observation is relevant only to the parameters used in this study, in which the maximal voltage was 1500 V (1000 V/cm voltage over distance) and the maximal time constant 148 ms.

The E2 protocol requires a special waveform comprised of an exponential decay shape with a steep decrease in voltage to values that will not induce an electrical discharge across the electrolytically product near the electrodes and a longer low voltage tail, that can generate sufficient products of electrolysis for the E2 ablation. To the best of our knowledge currently available electroporation systems cannot deliver exponential decay waveforms with the desired, electrolytic products generating time constants. To this end we have modified existing commercial designs (e.g. Gene Pulser Xcell™ Electroporation System, BioRad, Hercules, CA), as described in the methods and materials section. The key difference is the use of larger capacitance, in essentially the same circuit.

Our main criteria for evaluating the exponential decay voltage waveform ability to ablate tissue in a clinically significant manner was the ability to induce the ablation throughout the gap between the electrodes. Therefore, the histological and mathematical analysis is focused on the tissue found midway between the electrodes. This is the part of the treated tissue in which the lowest electric fields and lowest temperatures occur. Figures 1 and 2 show that there are parameters of initial voltage and time constant for which the tissue midway between the electrodes is not ablated. Figure 1A shows that for an initial voltage of 750 V and a distance of 1.5 cm between the electrodes (500 V/cm distance between electrodes), the electric field strength midway between the electrodes is lower than 200 V/cm. This value is substantially below the reversible electroporation threshold for the rabbit liver, which was measured to be 362 +/21 V/cm (Miklavcic et al. 2000). Since the calculated temperature midway between electrodes is below 40°C, there is no mechanism to induce damage between the electrodes. The conditions in the region between the electrodes are below the levels required for irreversible electroporation ablation, reversible electroporation or thermal ablation.

Figure 2 shows that increasing the initial voltage of the exponential decay waveform to 1000 V will also increase the extent of the damage near the electrodes. The distance between the electrodes is 1.5 cm and therefore the initial voltage to distance ratio is 750 V/cm. Figure 2E shows that the electric field midway between electrodes is calculated to be below 300 V/cm. This value is below the 362 +/- 21 V/cm reversible electroporation threshold (Miklavcic et al. 2000). Tissue damage by heat can be also excluded, since the temperature between electrodes does not exceed 40°C (Figure 1B and 2F). In this case also, the conditions in the middle between the electrodes are below the levels required for irreversible electroporation ablation, reversible electroporation or thermal ablation.

Figures 3 and 4 show that it is possible to ablate the entire zone between electrodes by using two consecutively delivered exponential decay waveforms with the same parameters as those used to produce the results in Figure 2. The initial voltage of the exponential decay waveform was 1000 V. The distance between the electrodes is 1.5 cm and therefore, the initial voltage to

distance ratio is 750 V/cm. The mechanism of ablation may be related to the possibility that the second exponential waveform has brought the tissue midway between electrodes to the threshold of E2 ablation. Figure 3F shows that the temperature prior to the delivery of the second exponential waveform is elevated relative to that prior to the delivery of the first waveform. Elevated temperatures favor electroporation and may reduce its threshold. Furthermore, it is known that electroporation changes the electrical conductivity of tissue. While Figure 3E was obtained for the electrical conductivity of the normal liver, the second waveform may generate a somewhat modified electric fields. Last, the second waveform has delivered twice the level of electrolytic compounds than in the experiment whose results are depicted in Figure 2. This tentatively suggests that the mechanism of tissue ablation in the middle part of the tissue between electrodes is the synergy between reversible electroporation and electrolysis.

The results displayed in Figures 5 and 6 produce stronger evidence of the E2 mechanism of tissue ablation. Here, an increase of the exponential decay waveform initial voltage to 1500 V has produce ablated tissue between the electrodes. Calculations show that the electric field midway between the electrodes is about 550 V/cm (Figure 5E). This value is below the irreversible electroporation threshold for the rat liver (637 V/cm +/- 43 V/cm)(Miklavcic et al. 2000). The temperature midway between electrodes is about 40°C, (Figure 5F), which is below the threshold of thermal damage. The mechanism of tissue ablation at the midpoint between electrodes is neither irreversible electroporation nor thermal. The most likely possible mechanism is the synergistic effect of electrolysis and reversible electroporation.

This is a first large animal study on the use of the synergy between electrolysis and reversible electroporation to enhance tissue ablation by electroporation. However, the E2 combination seems promising. It has the ability to create comparable clinically relevant areas of tissue ablation, in a much shorter period of time than irreversible electroporation, with lower voltages and single waveforms, without the need to inject drugs and without the need for paralyzing anesthesia.

Acknowledgements

We would like to thank Dr. Narayan Raju from Pathology Research Laboratory, Inc for his assistance on the pathological examination and analysis.

Author contributions statement

B.R. conceived the experiment, M.S., P.M., E.G., N.K. and B.R. conducted the experiment, E.G. B.R. and N.K. analyzed the results. All authors reviewed the manuscript.

References

Czymek, R., D. Dinter, S. Loeffler, M. Gebhard, T. Laubert, A. Lubienski, H.-P. Bruch and A. Schmidt (2011). "Electrochemical Treatment: An Investigation of Dose-Response Relationships Using an Isolated Liver Perfusion Model." Saudi Journal of Gastroenterology **17**(5): 335-342.

Davalos, R. V., L. M. Mir and B. Rubinsky (2005). "Tissue ablation with irreversible electroporation." Annals of Biomedical Engineering **33**(2): 223-231.

Guenther, E., N. Klein, P. Mikus, M. K. Stehling and B. Rubinsky (2015). "Electrical breakdown in tissue electroporation." Biochemical and Biophysical Research Communications **467**(4): 736-741.

Ivorra, A. and B. Rubinsky (2007). "In vivo electrical impedance measurements during and after electroporation of rat liver." Bioelectrochemistry **70**(2): 287-295.

Marty, M., G. Sersa, J. R. Garbay, J. Gehl, C. G. Collins, M. Snoj, V. Billard, P. F. Geertsen, J. O. Larkin, D. Miklavcic, I. Pavlovic, S. M. Paulin-Kosir, M. Cemazar, N. Morsli, Z. Rudolf, C. Robert, G. C. O'Sullivan and L. M. Mir (2006). "Electrochemotherapy - An easy, highly effective and safe treatment of cutaneous and subcutaneous metastases: Results of ESOPE (European Standard Operating Procedures of Electrochemotherapy) study." EJC Supplements **4**(11): 3-13.

Miklavcic, D., D. Semrov, H. Mekid and L. M. Mir (2000). "In vivo electroporation threshold determination." Proceedings of the 22nd Annual International Conference of the IEEE Engineering in Medicine and Biology Society (Cat. No.00CH37143): 2815-2818 vol.2814.

Mir, L. M., M. Belehradek, C. Domenge, S. Orlowski, B. Poddevin, J. J. Belehradek, G. Schwaab, B. Luboinski and C. Paoletti (1991). "Electrochemotherapy, a new antitumor treatment: first clinical trial." Comptes Rendus de l'Academie des Sciences Serie III Sciences de la Vie **313**: 613-618.

Nilsson, E., H. von Euler, J. Berendson, A. Thorne, P. Wersall, I. Naslund, A. S. Lagerstedt, K. Narfstrom and J. M. Olsson (2000). "Electrochemical treatment of tumours." Bioelectrochemistry **51**(1): 1-11.

Phillips, M., H. Krishnan, N. Raju and B. Rubinsky (2016). "Tissue ablation by a synergistic combination of electroporation and electrolysis delivered by a single pulse." Annals of Biomedical Engineering.

Phillips, M., N. Raju, L. Rubinsky and B. Rubinsky (2015). "Modulating electrolytic tissue ablation with reversible electroporation pulses." Technology **3**(1): 45-53.

Rubinsky, B., G. Onik and P. Mikus (2007). "Irreversible electroporation: A new ablation modality - Clinical implications." Technology in Cancer Research & Treatment **6**(1): 37-48.

Sale, A. J. H. and W. A. Hamilton (1967). "Effects of high electric fields on microorganisms. 1. Killing of bacteria and yeasts." Biochimica et Biophysica Acta **148**: 781-788.

Stehling, M. K., E. Guenther, P. Mikus, N. Klein, L. Rubinsky and B. Rubinsky (2016). "Synergistic Combination of Electrolysis and Electroporation for Tissue Ablation." Plos One **11**(2).

Initial Voltage U_0	750V (Fig.2), 1000V (Fig.3,4), 1500V (Fig.5)
Exposure length	1cm (Fig.2,3,4) 2cm (Fig.5)
Decay	Exponential capacitor discharge
Power supply capacitance	Listed in Figures
Distance between electrodes	1.5cm
Electrode diameter	1mm
Liver: electrical conductivity	0.286 S/m
Liver: heat capacity	3750 J/(kg*K)
Liver: density	1000 kg/m^3
Liver: thermal conductivity	0.52 W/(m*K)
Titanium: electrical conductivity	7.4e5 S/m
Titanium: heat capacity	710 J/(kg*K)
Titanium: density	4940 kg/m^3
Titanium: thermal conductivity k	7.5 W/(m*K)

Table 1: Parameters used for the thermal and electrical field calculations.

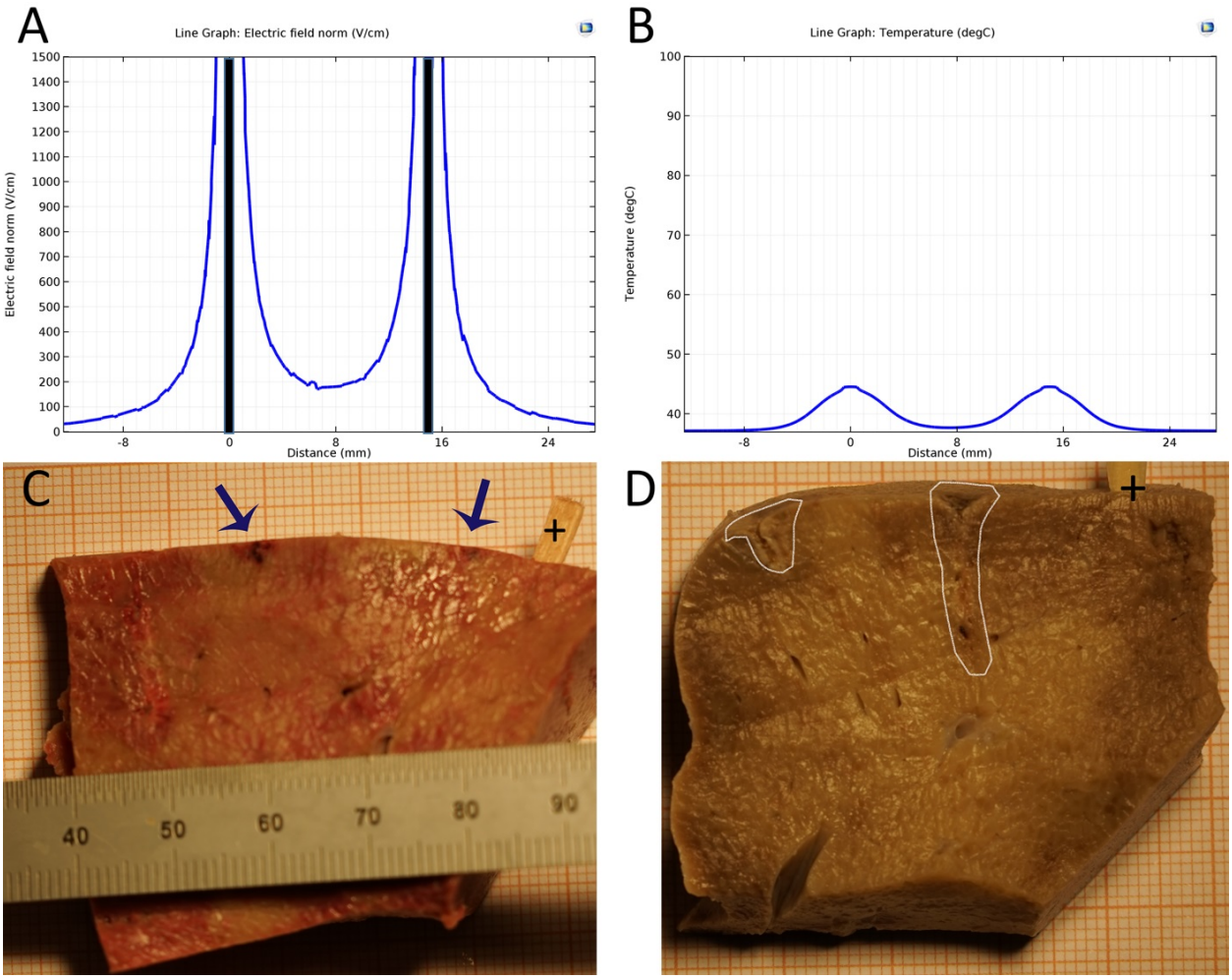

Figure 1: Study with an EDW with initial voltage difference between electrodes of 750 V and various time constants. **A.** calculated electric field. **B.** Calculated thermal field after 30 seconds. **C.** Macroscopic image - 50 ms time constant – no ablation was noticed. **D.** Macroscopic image - 100 ms time constant – some ablation near electrodes.

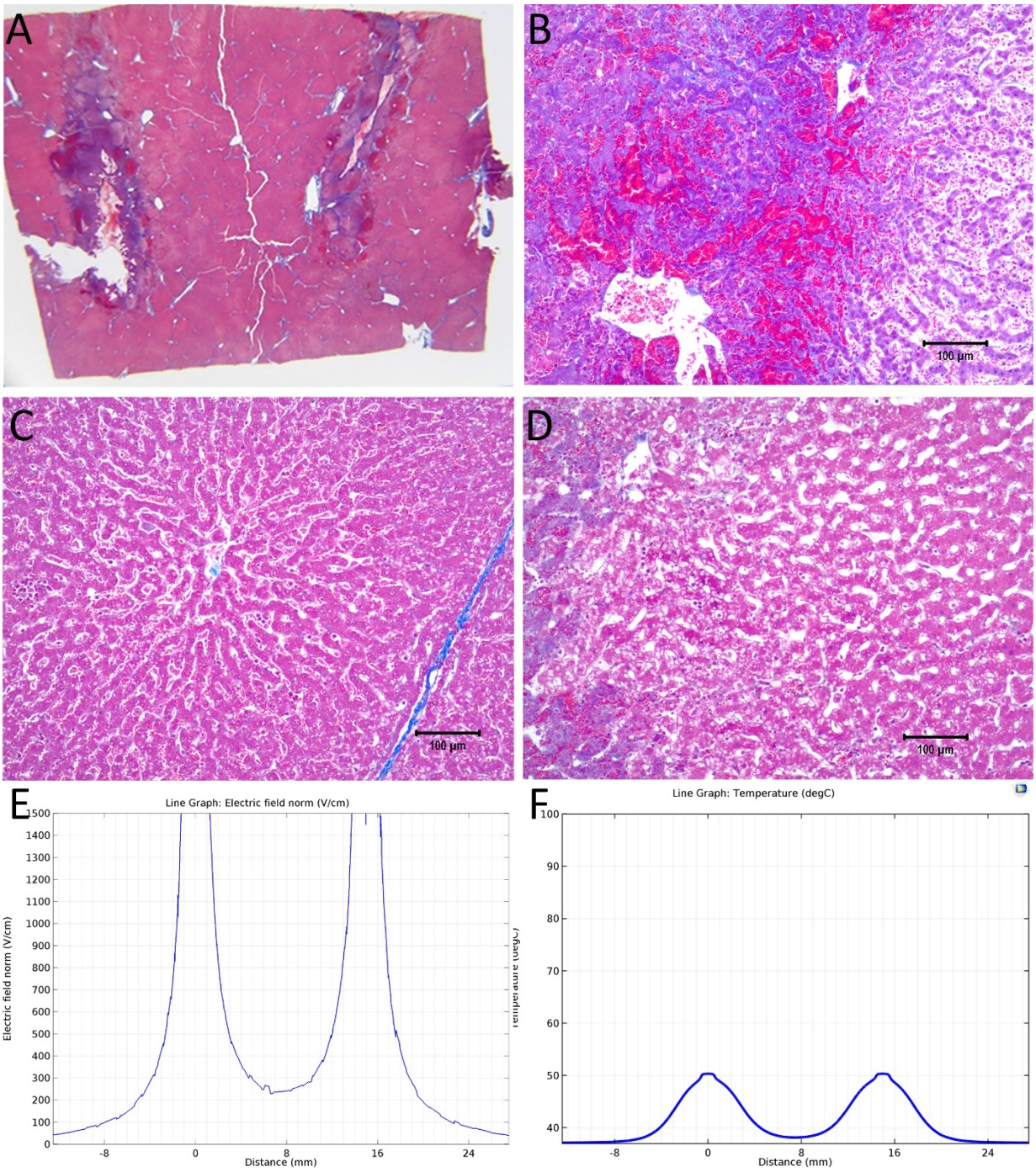

Figure 2: Study with one EDW with initial voltage difference between electrodes of 1000 V and time constant of 70 ms. **A.** Histological slide with Masson's trichrome staining. **B.** 10x magnification of the right lesion, which is the anode. We see severe acute hepatocellular necrosis with coagulated blood (hemorrhage) in the sinusoids. **C.** 10x magnification between the electrodes. The cells do not appear to be affected. **D.** 10x magnification at the margin of the left lesion, which is the cathode. Here we see the borderline between the necrotic tissue on the left and partially affected cells on the right. **E**. Electric field strength distribution. **F.** Temperature distribution after 30 seconds. (scale bar 100 µm)

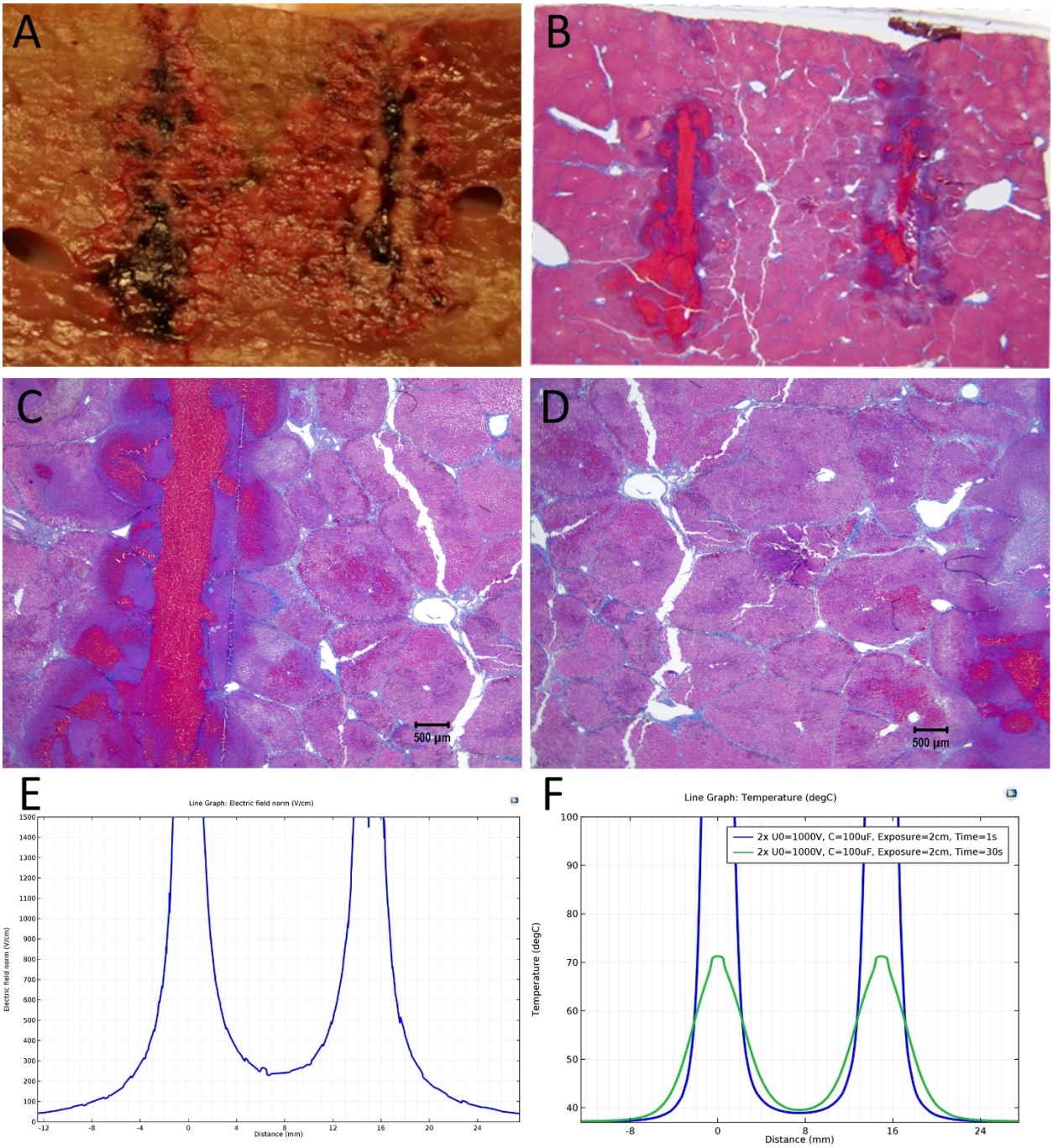

Figure 3: Study with 2 EDW separated by 30 s with time constants of 79 and 92 ms, the first and second pulse respectively, 1000 V difference between electrodes placed at a distance of 15 mm between them, 10 mm exposed length, 100 µF capacitor. Liver was extracted 18.5 h after treatment. **A.** Macroscopic histological slide (cathode left electrode anode right electrode) **B.** Masson's trichrome staining reveals blood coagulation (red) and ablation both around and in between electrodes. **C.** Close-up of the cathode, which is the left electrode. **D.** Close-up of the right electrode, which is the anode. (scale bar 500 µm) **E.** Electric field strength distribution. **F.** Temperature distribution prior to the delivery of the second waveform at 1 and 30 seconds.

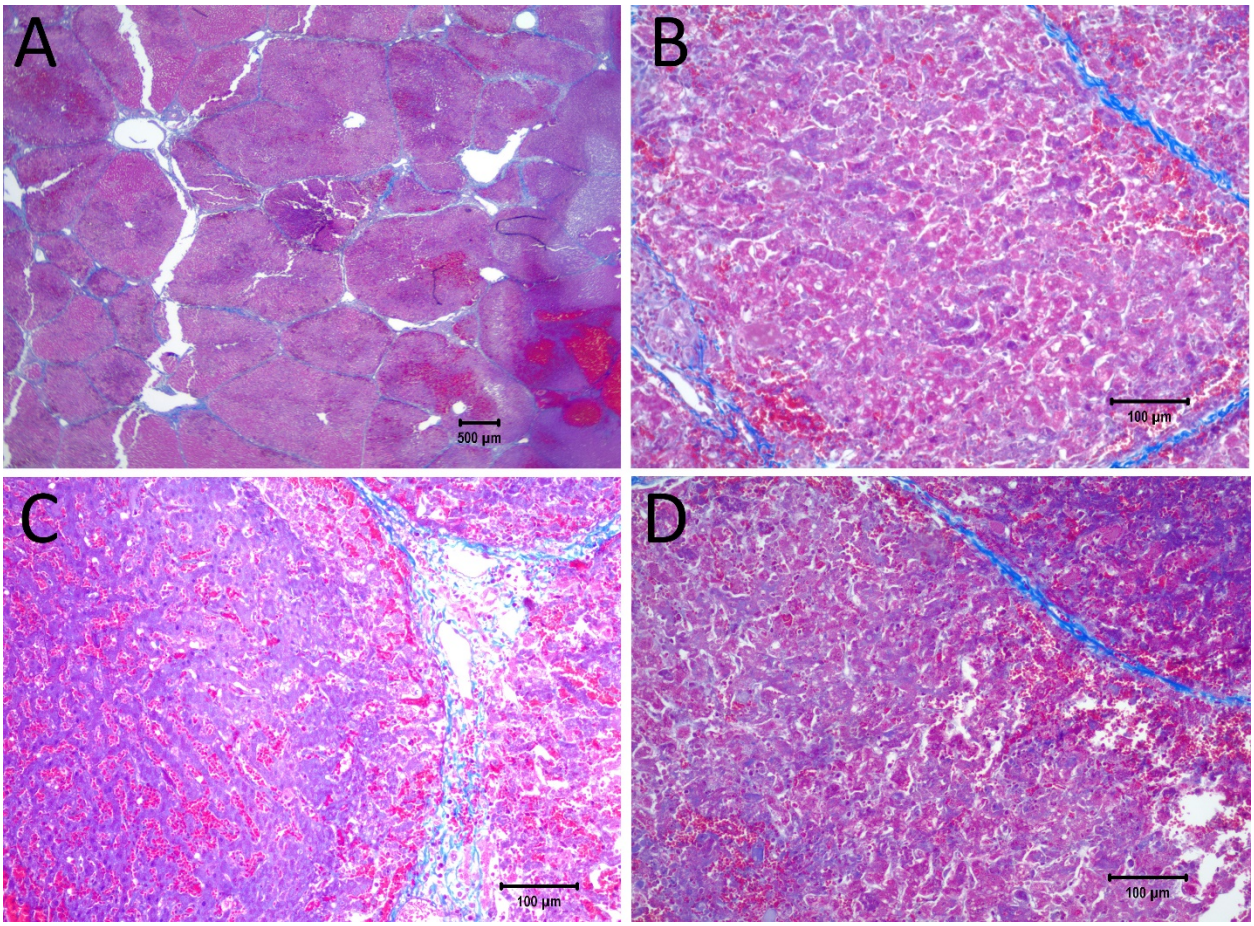

Figure 4: Details from Figure 3. **A.** Space between the electrodes in Figure 3. Bar indicates 500 µm. **B.** 10x magnification of cells between the electrodes, showing the details of the ablated area. **C.** 10x magnification of the cathode, showing edema and cellular ablation injury. **D.** 10x magnification of the area by the anode, showing the margin of affected and non-affected cells. All images show Masson's trichrome staining. Bars in B-D indicate 100 µm.

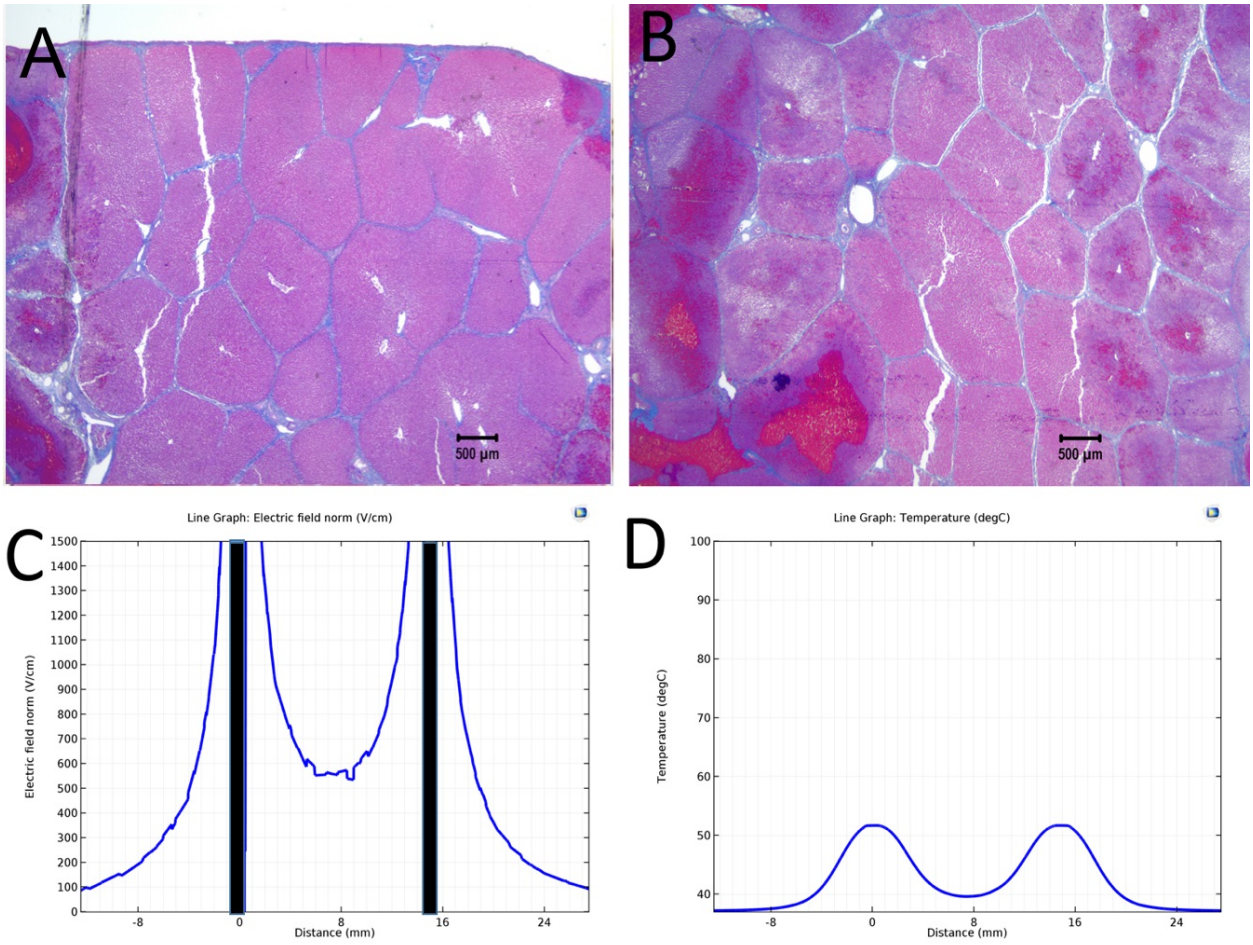

Figure 5: Study with a EDW with a time constant of 69 ms, 1500 V difference between electrodes placed at a distance of 15 mm between them, 200 mm exposed length, 100 µF capacitor. **A.** Macroscopic cross section in a plane through the axis of the electrodes. Image taken between electrodes at the part where the electrodes were insulated, showing that the cells are not affected. **B.** Image taken between electrodes where the electrodes were not insulated showing that the lesion was bridged. (500 µm bar). **C**. Electric field strength distribution. **D.** Temperature distribution after 30 seconds.

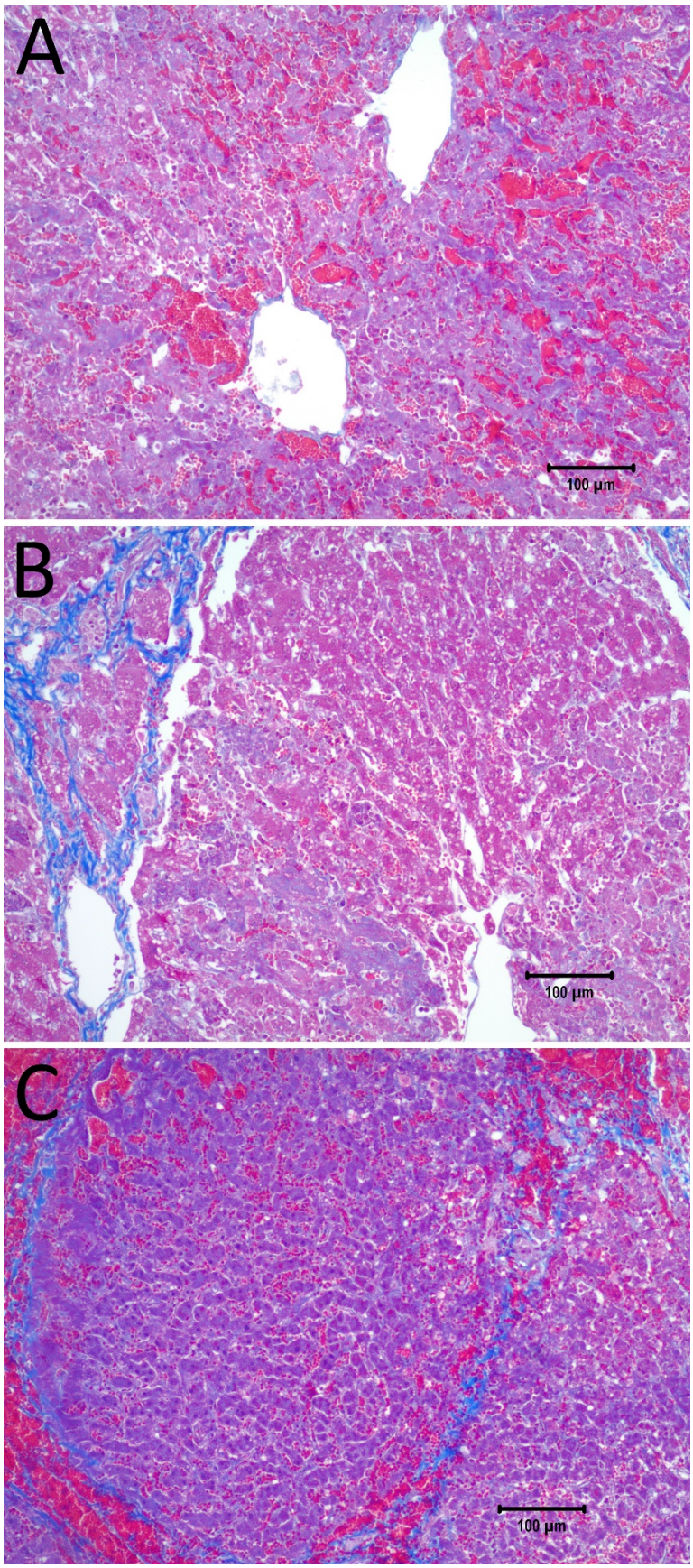

478

Figure 6: 10x magnification of the pathological slides shown in Fig 5. **A.** Image taken at the right electrode, which was the cathode, showing necrotic, swollen hepatocytes and a disrupted sinusoidal pattern. **B.** Image taken between the electrodes, illustrating a complete loss of cellular structure with swollen hepatocytes. **C.** Left electrode, which was the anode, showing an affected cellular architecture and hemorrhage. Note that the large blood vessels are open and unaffected. Scale bar 100 µm